ISSN 0742-0463, Journal of Volcanology and Seismology, 2014, Vol. 8, No. 6, pp. 411–417. © Pleiades Publishing, Ltd., 2014.

Volcanic Eruption Trends in the Five-Years Pre-Eruption Era[1]

M. E. Emetere

Department of Physics, Covenant University Canaan land, P.M.B 1023, Ota, Nigeria
e-mail: moses.emetere@covenantuniversity.edu.ng

Abstract—Predicting volcanic eruption and magmatic transports is a global research. In this study, the temperature deviation curve model and temperature polynomial expansion scheme was used to calculate the time-scale of an active pre-eruption process. Satellite imagery within the timescale was harvested to further corroborate the findings.

DOI: 10.1134/S0742046314060086

INTRODUCTION

The mechanism of volcanic systems are highly unpredictable [1] because of the different features of the earth crust at each volcanic zones, shape and sizes of the magma reservoir. There are numerous hypotheses or models for detecting and predicting volcanic prone regions but salient parameters have been ignored. The main hypotheses are centered on the geophysical, geothermal and geochemical techniques. They include the Failure Forecast Method (FFM) [2] and Thermal remote sensing (TRS). FFM and TRS have been used to predict eruptions at short notices i.e. within hours or days. The diversity of research has shown that dependence on one technique may be unreliable at the moment [3–7]. This suggests that more multidisciplinary efforts are required to proffer accurate prediction.

Volcanic zones are characterized by many factors but the major is the magmatic features. Magma stored in chambers/mushes is surrounded by crustal rocks. Magma bodies are open systems or self-organized dissipative structures that exchange material and heat with their surroundings under far-from-equilibrium conditions. The massive magma chamber transmits heat flux by conduction through the crust rocks to the ascending soil layer and by convection through the conduits via the pores/cracks of the soil layer. The transmitted heat flux via different media creates series of surface pattern. An advanced heat flux accumulation about a region-having a homogenous media, leads to ground inflation [8]. Heat flux pattern depends on the sizes and number of magma chambers; it acts like a photographic film that captures series of events in the high temperature geothermal fields close to the magma reservoir [22]. Therefore, it is scientifically valid to propose that heat flux pattern from within the earth-crust differs due to thermal conductivity of the soil layer. The long wave radiation from the earth is ignored because of its non-uniformity within regions of equal climatic signatures. The gas flux is an advanced stage of the heat flux transmission within the eruption timescale. Ultimately, the gas flux ejection determines the most prospective conduit for eruption.

In our model, Soil heat flux is the major factor used for calculating the timescale of pre-eruption era. Different techniques-both theoretical and experimental have been employed to estimate soil heat flux and its implication at different magnitude. Among the reliable theoretical methods for estimating soil heat flux is the Temperature Deviation Curve Model (TDCM). The TDCM has been used to predict the susceptibility of Abuja metropolis to soil compaction [9]; determine the annual amplitude of the surface soil temperatures of the same region [9]; estimate soil heat flux from both short and long-term remotely sensed surface temperature [10]; monitor earthquakes [11]; derive the temperature polynomial expansion scheme for sensible heat flux [12]; forecast hydrological disaster [13].

So far, literatures have only accounted for conductive heat transport from the top soil to the subsurface [14–16]. The reverse seem to be difficult because we have to account mathematically a conductive model-capable of transmitting within several kilometers from the magma chamber to about fifteen meters below the top soil. In this paper, we propose via an in-depth mathematical experimentation that the duration between the heat flux and the gas flux is about five years; and the duration between the gas flux ejection and eruption is about a year. Our main objective is improving on the geothermal technique to forecast volcano eruption at longer notices.

[1] The article is published in the original.

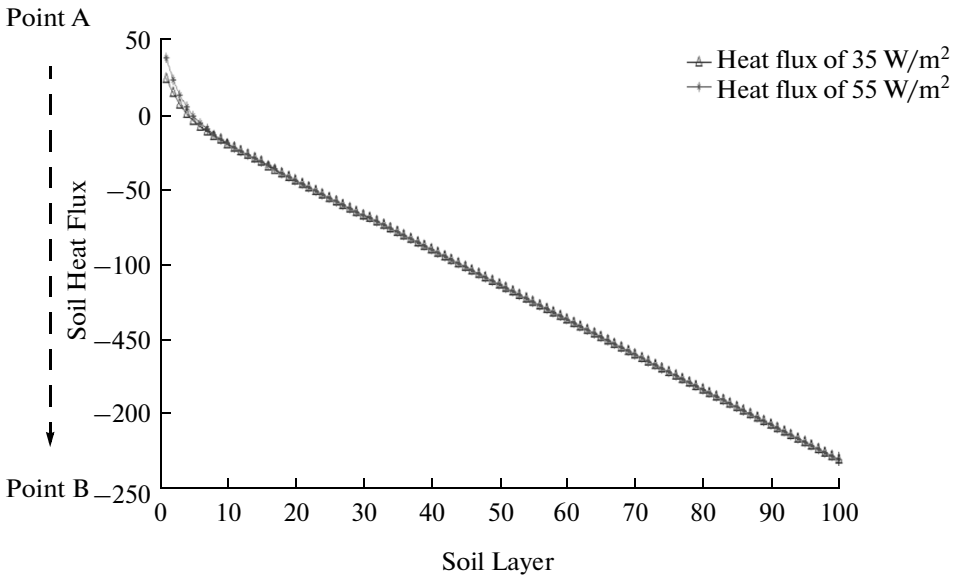

Fig. 1. Soil heat flux trend within multiple soil layer.

MATHEMATICAL DERIVATION OF THE TIMESCALE PRE-ERUPTION MODEL

In this section, the objective is to calculate the timescale from the point of eruption to the point the magma contents are excited within chamber. To do that, we start with the climax-before eruption (point A) to about 10 km below the earth crust (point B). At point A, the eruption is characterized with volcanic-tremor [15] or earthquake [16]. The magnitude of the earthquake with respect to the behavioral component of the soil properties [6] had been estimated to be

$$M = \frac{2}{3}\log\left(\frac{k^2}{2\omega}\right)\left(\frac{\rho_s}{\rho_b}\right)^2 - 7.87, \quad (1)$$

where K is the hydraulic conductivity, M is the magnitude of the earthquake, ρ_s is the soil particle density, ρ_b is the soil bulk density, ω is the circular frequency and k is the thermal diffusivity.

Between point A and B, are soil layers, rocks, aquifer e.t.c. which are subject to changing temperature. We therefore introduce the temperature deviation curve model [9] to account for the thermal instability. It is written as

$$\Delta T = A_0 e^{-\rho_s/\rho_b}\sin\left(-\frac{\rho_s}{\rho_b} - \frac{\pi}{2}\right), \quad (2)$$

where ρ_s = soil particle density which is a approximately 2.66 g cm^{-3} by Gupta et al. [17], ρ_b = soil bulk density. Since the change of the temperature is with respect to time, equation is written as

$$\frac{\partial T_1}{\partial t} = A_0 e^{-\rho_s/\rho_b}\sin\left(-\frac{\rho_s}{\rho_b} - \frac{\pi}{2}\right). \quad (3)$$

Earlier, the heat flux had been reported [10] to follow a polynomial trend in a uni or multi soil layer.

$$\begin{cases} G_n = \frac{2^n}{3} G_0 \ \text{ for } \ n \le 1 \\ G_n = \left(\frac{2}{3}\right)^n G_0 - \frac{7}{3(n-1)} \ \text{ for } \ n \ge 2. \end{cases} \quad (4)$$

The more the soil layer, the lower the soil heat flux. This idea is in line with common physics principles. Therefore, Eq. (4) shall be used in calculating an assumed 100 layers. The numerical analysis when $G_0 = 35$ W/m^2 at the 100th layer showed the highest positive heat fluxes i.e. G_n = 23.45, 13.38, 5.86, 0.053 W m^{-2}. Figure 1 shows that the magnitude of the heat flux transport at the magma chamber flows at a peculiar—trend regardless the boundary barriers within the earth crust. However, due to the implications of Eqs. (1) and (2) the heat flux varied due to densities of the earth crust content and attenuations from atmospheric net radiation impact. The uneven arrival of the heat flux at point B gives the pictorial patterns of occurrences within the crust.

The downward propagating temperature signal as a function of time (t) and depth (z) is given by Carslaw and Jaeger [18] as

$$T(z, t) = Ae^{-Kz}\cos(\omega t + \epsilon - Kz). \quad (5)$$

Fig. 2. Satellite location of Eyjafjallajökull and Mount Merapi (Retrieved from NASA web).

During heat flux transport, the change of the temperature is with respect to time. Therefore the Eq. (5) is written

$$\frac{\partial T_2}{\partial t} = Ae^{-Kz}\cos(\omega t + \epsilon - Kz), \tag{6}$$

where $T_2 = T(z, t)$, $T_1 = T(\rho_s, 0)$. Equation (6) is the attenuation thermal factor by the atmospheric net radiation.

The combined rate of change of temperature that is equivalent to the resultant heat flux close to point B can be summarized as

$$\frac{\partial T}{\partial t} = \frac{\partial T_1}{\partial t} - \frac{\partial T_2}{\partial t}, \tag{7}$$

$$\frac{\partial T}{\partial t} = A_0 e^{-\rho_s/\rho_b}\sin\left(-\frac{\rho_s}{\rho_b} - \frac{\pi}{2}\right) - Ae^{-Kz}\cos(\omega t + \epsilon - Kz). \tag{8}$$

On the assumption that $\epsilon = 0$ and $\frac{\rho_s}{\rho_b} = Kz$, the trigonometry technique is applied to expand Eq. (8)

$$\frac{\partial T}{\partial t} = e^{-Kz}\left[A_0\cos\left(\frac{\rho_s}{\rho_b}\right) - A\cos(\omega t)\cos(kz) + A\sin(\omega t)\sin(kz)\right]. \tag{9}$$

Therefore applying the soil heat transfer theory [19]

$$G(0, t) = \Delta T_0 (C\omega\gamma)^{0.5}\sin(\omega t + \pi/4). \tag{10}$$

where $G(0, t)$ = instantaneous surface soil heat flux density (W m^{-2}); T_0 = the amplitude of the surface temperature (°C) wave $(T_{max} - T_{min})/2$, t = time of day (s); λ = the soil thermal conductivity (W m^{-1} K^{-1}); C = the volumetric heat capacity (J m^{-3} K^{-1}) ω = frequency.

The characteristic of the soil heat transfer can be written as

$$G(0.t) = \frac{\partial T}{\partial t}(C\omega\gamma)^{0.5}\sin(\omega t + \pi/4). \tag{11}$$

Applying (9) into (11) suggests roughly that the timescale of thermal signals between point A and B is approximately 5.8 yr. We narrowed down our research on the satellite imaging over two volcanic sites within 2010 to ascertain our calculations.

APPLICATION OF THE THERMAL ASCENSION MODEL

Our research focus is the two volcano eruptions recorded in 2010 i.e. Eyjafjallajökull and Mount Merapi as shown in Fig. 2. The Eyjafjallajökull volcano erupted twice in 2010 i.e. less than two months. The last volcanic eruption before 2010 occurred twice within eighteen months i.e. between 1821 and 1823. On the other hand, the mount Merapi is an active stratovolcano which erupts regularly. The last eruption occurred in 2006.

Figure 3 according to our calculation is the birth of a volcanic process triggered by the magma excitations

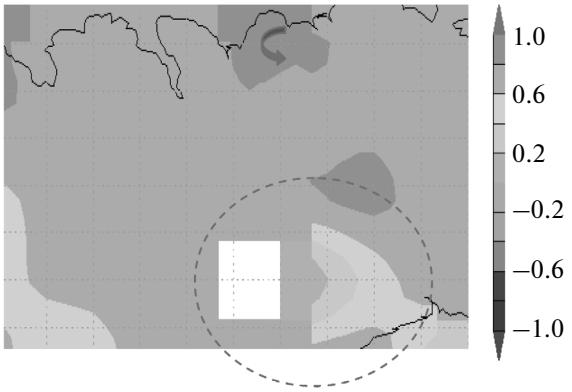

Fig. 3. Eyjafjallajökull-Downward heat flux at base of soil top layer 2005.

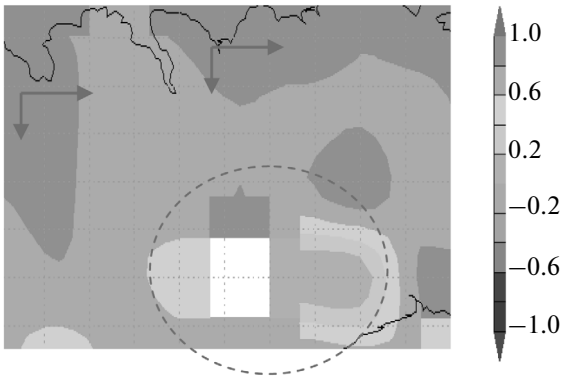

Fig. 4. Eyjafjallajökull-Downward heat flux at base of soil top layer 2006.

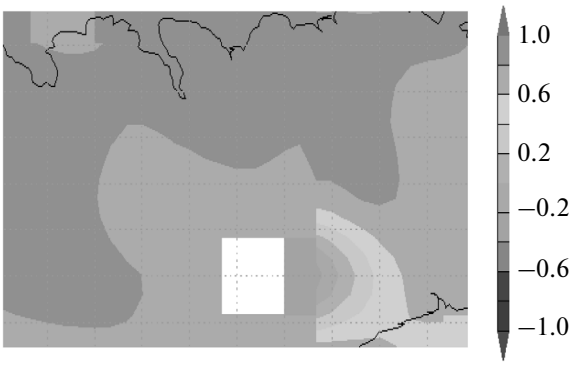

Fig. 5. Eyjafjallajökull-Downward heat flux at base of soil top layer 2007.

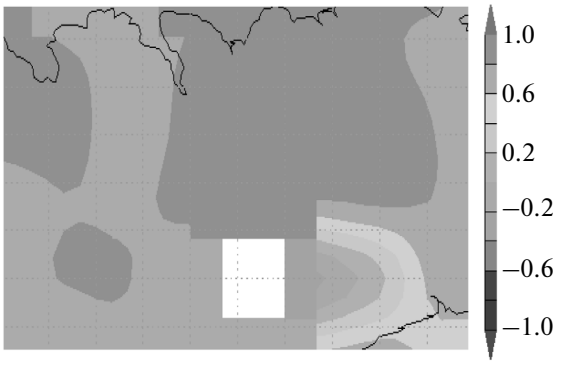

Fig. 6. Eyjafjallajökull-Downward heat flux at base of soil top layer 2008.

within the chamber. At this point, it starts emitting heat noticeable at distances beyond the eruption point (within the red circle). Up above the red circle, the heat flux starts gaining magnitude with a gradual spread (Fig. 4).

The mechanism for heat transfer in Eq. (4) is majorly hydrothermal convection. The heat flux flows in a two dimensional pattern towards the red circle. Usually, magma reserviors-especially the basaltic volcano is developed with their centers at depths where magmas are neutrally buoyant in the surrounding crust [20]. Within the red circle (we call the action point), there is an expansion of the magma chamber [21]. This phenomenon has been explained by scientist as the release of fresh magma into existing magma body. The heat flux keeps spreading to towards its source (Fig. 5) while the source contracts due to the presence of aquifers (blue box). The heat flux is lowered because of the contraction and starts moving away from the "action point" (see Fig. 6).

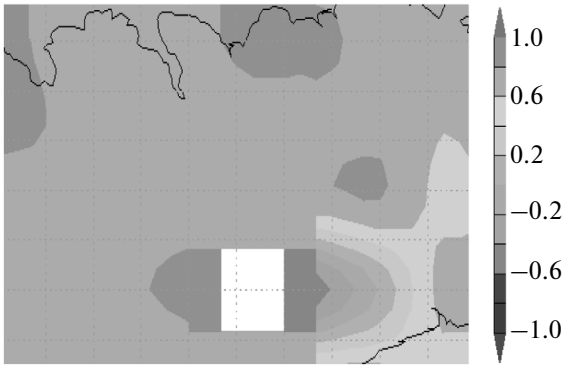

Fig. 7. Eyjafjallajökull-Downward heat flux at base of soil top layer 2009.

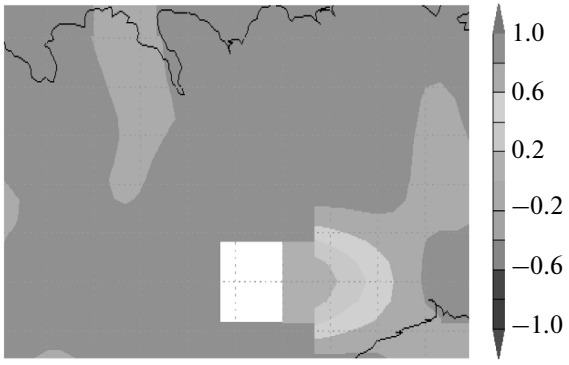

Fig. 8. Eyjafjallajökull-Downward heat flux at base of soil top layer 2010.

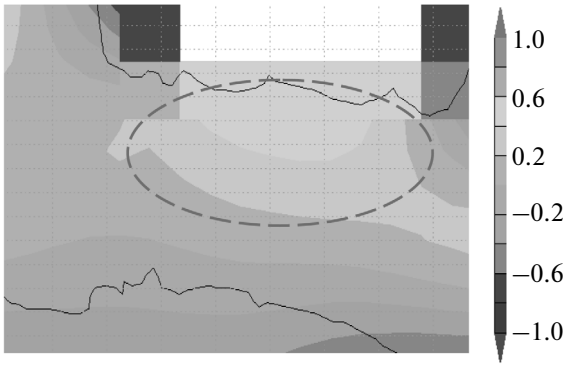

Fig. 9. Mount Merapi-Downward heat flux at base of soil top layer 2005.

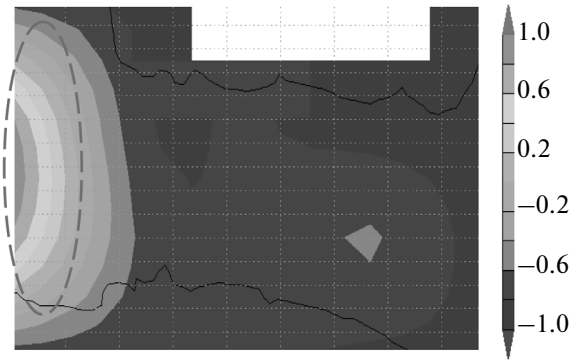

Fig. 10. Mount Merapi -Downward heat flux at base of soil top layer 2006.

The gas flux is released (Fig. 7) at the "action point". The action point is the likely spot within a defined area—where the hot volcano will erupt.

The chamber uniformly expands until the eruption occurred in 2010 (Fig. 8). The two volcanic eruptions which took place same year (within 2010) may be because of a large aquifer intersections on the magma flow paths. The heat flux extends from the source and spreads abroad the regions.

The second case is the Mount Merapi. The mechanism of heat transport is basically via heat conduction into the walls of the rock as shown in Figs. 9–14. The heat flux as shown in Figs. 9–14 was minimum and the gas flux maximum at the "action point" (Fig. 9). Like the theory-propounded in Eyjafjallajökull, Fig. 10 showed the presence of volcanic eruption. Unlike the Eyjafjallajokull experience, the earth crust may possess voids which allow some of the magma to relocate as shown in the Fig. 10. The causes of the magma relocation (whether dykes or ordiapiric) is not among the objective of this paper.

The relocated magma chamber transports heat towards the earth surface (Fig. 11). The magma splits into two (Fig. 12) and transports heat from two spots (Fig. 13). This is one of the characteristics of an open system i.e. they have many degrees of freedom. The two spots (Fig. 13) and its corresponding magma growth are the sources of the notable volcano eruption which occurred twice within a short time

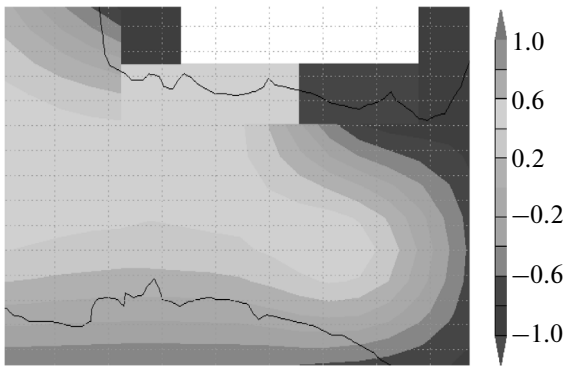

Fig. 11. Mount Merapi-Downward heat flux at base of soil top layer 2007.

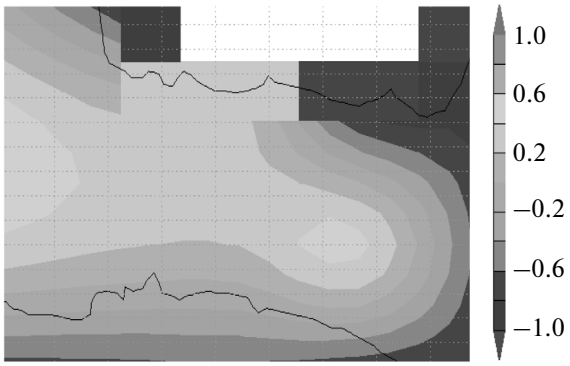

Fig. 12. Mount Merapi-Downward heat flux at base of soil top layer 2008.

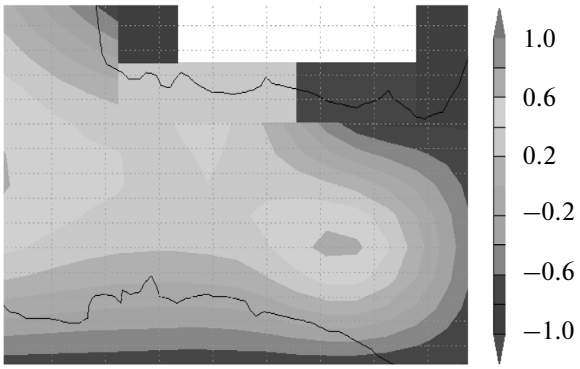

Fig. 13. Mount Merapi-Downward heat flux at base of soil top layer 2005.

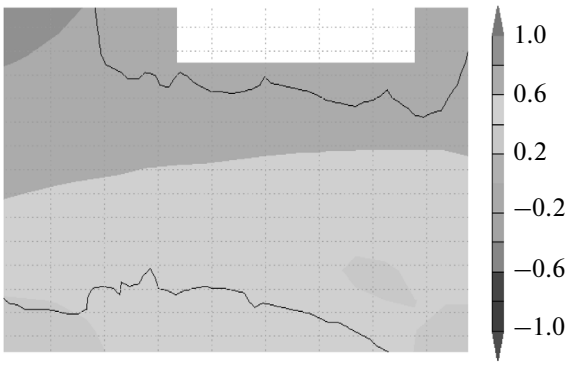

Fig. 14. Mount Merapi-Downward heat flux at base of soil top layer 2006.

interval. This phenomenon explains the frequent volcanic eruption in Mount Merapi.

CONCLUSIONS

The five year pre-eruption era via our calculation seem to offer solution towards predicting volcanic eruption for at least five years. The importance of the geothermal analysis to forecast volcanic eruption cannot be under estimated via salient discoveries-shown in this paper. Therefore it safe to ask this question. Can volcanic sites be relocated? Perhaps this theory may supply answers upon further investigation.

ACKNOWLEDGMENTS

The author appreciates NASA for using their satellite imagery.

REFERENCES

1. Melnik, O. and Sparks, R.S.J., Nonlinear dynamics of lava extrusion, *Nature*, 1999, vol. 402, pp. 37–41.
2. Voight, R. and Cornelius, R., Prospects for eruption prediction in near-real-time, *Nature*, 1991, vol. 350, pp. 695–698.
3. Annen, C. and Sparks, R.S.J., Effects of repetitive emplacement of basaltic intrusions on thermal evolution and melt generation in the crust, *Earth Planet. Sci. Lett.*, 2002, vol. 203, pp. 937–955.
4. De Saint-Blanquat, M., Habert, G., Horsman, E., Morgan, S.S., Tikoff, B., Launeau, P., and Gleizes, G., Mechanisms and duration of nontectonically assisted magma emplacement in the upper crust: the Black Mesa pluton, Henry Mountains, *Utah. Tectonophysics,* 2006, vol. 428, pp. 1–31.
5. Costa, F., Chakraborty, S., and Dohmen, R., Diffusion coupling between trace and major elements and a model for calculation of magma residence times using plagioclase, *Geochim. et Cosmochim. Acta*, 2003, vol. 67, pp. 2189–2200.

6. Dimalanta, C., Taira, A., Yumul G.P., Jr., Tokuyama, H., and Mochizuki, K., New rates of western Pacific island arc magmatism from seismic and gravity data, *Earth Planet. Sci. Lett.*, 2002, vol. 202, pp. 105–115.
7. Karlstrom, L., Dufek, J., and Manga, M., Magma chamber stability in arc and continental crust, *J. Volcan. Geotherm. Res.*, 2010, vol. 190, pp. 249–270.
8. Lu, Z., Mann, D., Freymueller, J.T., and Meyer, D.J., Synthetic aperture radar interferometry of Okmok volcano, Alaska: radar observations, *J. Geophys. Res.*, 2000, vol. 105, pp. 10791–10806.
9. Uno, E.U., Emetere, M.E., and Adelabu, J.S., Parametric investigation of soil susceptibility to compaction using temperature deviation curves, *Sci. J. Civil Eng. Architect.*, 2012, no. 2, pp. 1–6.
10. Uno, E.U., Emetere, M.E., and Eneh, Daniel, C.D., Simulated analysis of soil heat flux using temperature deviation model, *Sci. J. Phys.*, 2012, no. 2, pp. 1–9.
11. Emetere, M.E., Monitoring and prediction of earthquakes using simulated temperature deviation curve model, *Int. J. Appl. Inform. Systems*, 2012, vol. 4, no. 3, pp. 13–17.
12. Uno, E.U. and Emetere, M.E., *Analysing the impact of soil parameters on the sensible heat flux using simulated temperature curve model*, *Int. J. Phys. Res.*, 2012, vol. 2, no. 4, pp. 1–9.
13. Uno, E.U., Emetere, M.E., and Abdulrahman, U.U., Parametric analysis of ground temperature profile in Bwari-North Central Nigeria, *J. Environ. Earth Sci.*, 2013, vol. 3, no. 5, pp. 155–160.
14. Jason, E.S., Henry, N.P., John, W.E., and Matthew, J.L., Conduction-dominated heat transport of the annual temperature signal in soil, *J. Geophys. Res.*, 2003, vol. 108, p. 2431.
15. Hagerty, M.T., Schwartz, S.Y., Garces, M.A., and Protti, M., Analysis of seismic and acoustic observations at Arenal volcano, Costa Rica, 1995–1997, *J. Volcanol. Geotherm. Res.*, vol. 101, pp. 27–65.
16. Sparks, R.S.J., Forecasting volcanic eruptions, *Earth Planet. Sci. Lett.*, vol. 210, pp. 1–15.
17. Gupta, V.R. and Jangid, R.A., The effect of bulk density on emission behaviour of soil at microwave frequencies, *Int. J. Microwave Sci. Tech.*, 2011, vol. 160129, pp. 1–6.
18. Carslaw, H.S. and Jaeger, J.C., *Conduction of Heat in Solids*, 2nd ed., New York: Oxford Univ. Press, 1959, p. 510.
19. Sellers, W.D., *Physical climatology*, Chicago: The Univ. of Chicago press, 1965.
20. Ryan, M.P., *In Magmatic Processes: Physico-Chemical Principles*, 1987, p. 259.
21. Petford, N., Cruden, A.R., McCaffrey, K.J.W., and Vigneresse, J.L., Granite magma formation, transport and emplacement in the Earth's crust, *Nature*, 2000, vol. 408, pp. 669–673.
22. Moses E Emetere (2014). Forecasting Hydrological Disaster Using Environmental Thermographic Modeling. Advances in Meteorology 2014,783718.